Cerenkov Radiation–Induced Photoimmunotherapy with ^{18}F-FDG

Yuko Nakamura[1], Tadanobu Nagaya[1], Kazuhide Sato[1], Shuhei Okuyama[1], Fusa Ogata[1], Karen Wong[1], Stephen Adler[2], Peter L. Choyke[1], and Hisataka Kobayashi[1]

[1]*Molecular Imaging Program, Center for Cancer Research, National Cancer Institute, Bethesda, Maryland; and* [2]*Clinical Research Directorate/Clinical Monitoring Research Program, Leidos Biomedical Research, Inc., National Cancer Institute Campus at Frederick, Frederick, Maryland*

Near-infrared photoimmunotherapy (NIR-PIT) is a new cancer treatment that combines the specificity of antibodies for targeting tumors with toxicity induced by photoabsorbers after irradiation with NIR light. A limitation of NIR-PIT is the inability to deliver NIR light to a tumor located deep inside the body. Cerenkov radiation (CR) is the ultraviolet and blue light that is produced by a charged particle traveling through a dielectric medium faster than the speed of light in that medium and is commonly produced during radioactive decay. Here, we demonstrate the feasibility of using CR generated by ^{18}F-FDG accumulated in tumors to induce photoimmunotherapy. **Methods:** Using A431-luc cells, we evaluated the therapeutic effects of CR-PIT in vitro and in vivo using bioluminescence imaging. **Results:** CR-PIT showed significant suppression of tumor size, but the decrease of bioluminescence after CR-PIT was not observed consistently over the entire time course. **Conclusion:** Although CR-PIT can induce tumor killing deep within body, it is less effective than NIR-PIT, possibly related to the relatively lower efficiency of short wavelength light than NIR.

Key Words: photoimmunotherapy; UV-A light; Cerenkov radiation; ^{18}F-FDG

J Nucl Med 2017; 58:1395–1400
DOI: 10.2967/jnumed.116.188789

Near-infrared photoimmunotherapy (NIR-PIT) is a newly developed cancer treatment that combines the specificity of antibodies for targeting tumors with toxicity induced by photoabsorbers, for example, IRDye700DX (IR700, silica-phthalocyanine dye), after irradiation with NIR light (*1*). This induces nearly immediate necrotic cell death due to photo-induced cellular membrane damage (*1,2*). The first-in-human phase 1 trial of NIR-PIT in patients with inoperable head and neck cancer targeting epidermal growth factor receptor started in June 2015 (https://clinicaltrials.gov/ct2/show/NCT02422979) and has now advanced to a phase 2 trial in the United States. Although NIR light can penetrate several centimeters within tissue, an inherent limitation of NIR-PIT is the inability to deliver NIR light directly to a tumor deep within the body (*3,4*).

IR700 is a phthalocyanine derivative that typically has a narrow high absorbance in the deep red or near infrared, known as the Q-band, and is used for exciting IR700 in NIR-PIT. However, phthalocyanine derivatives, including IR700, have another broad intermediate absorbance peak at around 350 nm (ultraviolet [UV]-A or UV-B) (https://www.licor.com/bio/products/reagents/irdye/700dx/index.html), also known as the Soret-band, that can be an additional potential way to excite IR700 (Fig. 1).

Cerenkov radiation (CR) is the UV and blue light that is produced by a charged particle traveling through a dielectric medium faster than the speed of light in that medium and is commonly produced during radioactive decay (*5,6*). CR has been used for Cerenkov luminescence imaging, which pairs the production of visible light from radiotracers such as ^{18}F and ^{131}I with widely used small-animal optical imaging equipment (*6–12*).

The most widely used tracer is the ^{18}F-labeled analog of glucose, ^{18}F-FDG, which accumulates in metabolically active cells—such as those in the brain, the heart, or a malignant tumor—at a higher rate than other tissues (*13*). CR generated by ionizing radiation has been reported to excite IR700 (*14*). Taken together, tumors located deep in the body could potentially be treated by photoimmunotherapy induced by ^{18}F-FDG CR.

The purpose of this study was to determine whether CR generated by ^{18}F-FDG could induce photoimmunotherapy in a mouse tumor model.

MATERIALS AND METHODS

Reagents

IRDye 700DX succinimidyl ester was obtained from LI-COR Bioscience. Panitumumab, a fully humanized IgG_2 monoclonal antibody directed against epidermal growth factor receptor, was purchased from Amgen. Trastuzumab, 95% humanized IgG_1 monoclonal antibody directed against human epidermal growth factor receptor type 2 (HER2), was purchased from Genentech. All other chemicals were of reagent grade.

Synthesis of IR700-Conjugated Panitumumab and Trastuzumab

Panitumumab or trastuzumab (1 mg, 6.8 nmol) was incubated with IR700 succinimidyl ester (60.2 μg, 30.8 nmol) in 0.1 mol/L Na_2HPO_4 (pH 8.6) at room temperature for 1 h. The mixture was purified with a Sephadex G25 column (PD-10; GE Healthcare). The protein concentration was determined with a Coomasie Plus protein assay kit (Thermo Fisher Scientific Inc.) by measuring the absorption at 595 nm with spectroscopy (8453 Value System; Agilent Technologies).

Received Dec. 18, 2016; revision accepted Apr. 3, 2017.
For correspondence or reprints contact: Hisataka Kobayashi, Center for Cancer Research, National Cancer Institute, National Institutes of Health, Bldg. 10, Rm. B3B69, MSC1088, Bethesda, MD 20892-1088.
E-mail: kobayash@mail.nih.gov
Published online Apr. 13, 2017.

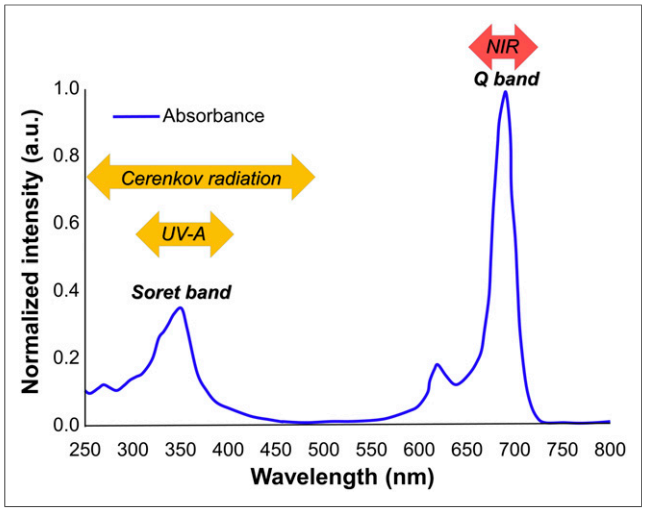

FIGURE 1. Absorption spectrum of IRDye 700DX.

The concentration of IR700 was measured by the amount of absorbance at 689 nm with spectroscopy to confirm the number of fluorophores conjugated to each monoclonal antibody. The synthesis was controlled so that an average of 2 IR700 molecules were bound to a single antibody. We abbreviate IR700 conjugated to panitumumab as pan-IR700 and to trastuzumab as tra-IR700.

Cell Culture

Epidermal growth factor receptor and luciferase-expressing A431-luc (epidermoid carcinoma of skin/epidermis) and MDAMB468-luc (adenocarcinoma of breast), and HER2 and luciferase-expressing 3T3/HER2-luc cells (fibroblast of embryo) were established. Cell lines were grown in RPMI 1640 (Life Technologies) supplemented with 10% fetal bovine serum and 1% penicillin-streptomycin (Life Technologies) in tissue culture flasks in a humidified incubator at 37°C in an atmosphere of 95% air and 5% carbon dioxide.

In Vitro UV-A PIT

Most CR is in the UV and blue end of the visible spectrum (*6*). Thus, first we determined the cytotoxic effects of UV-A PIT with pan-IR700 for A431-luc and MDAMB468-luc cells or tra-IR700 for 3T3/HER2-luc cells using flow cytometric propidium iodide (PI) (Life Technologies) staining, which can detect compromised cell membranes. Two hundred thousand cells were seeded into 12-well plates and incubated for 24 h. Medium was replaced with fresh culture medium containing 10 μg/mL of pan-IR700 or tra-IR700 and incubated for 6 h at 37°C. After the medium was washed with phosphate-buffered saline (PBS), PBS was added and cells were irradiated with a UV-A lamp, which emits light at a 365-nm wavelength with 1,090 μW/cm^2 (Spectroline E-series handheld lamps; Spectronics Corp.). Applied time was 0, 25, 50, 100, 200, 400, 800, and 1,600 s for 0, 0.025, 0.05, 0.1, 0.2, 0.4, 0.8, and 1.6 J/cm^2, respectively. Cells were scratched 1 h after treatment. Then PI was added in the cell suspension (final, 2 μg/mL) and incubated at room temperature for 30 min, followed by flow cytometry using a flow cytometer (FACS Calibur; BD BioSciences) and CellQuest software (BD BioSciences). To evaluate the killing of A431-luc cells with UV-A light, we calculated Δ percentage of surviving cells, based on the ratio of surviving cells exposed to UV-A light with or without pan-IR700 to those not exposed to UV-A light with or without pan-IR700.

In Vitro CR-PIT with ^{18}F-FDG

We examined the cytotoxic effects of in vitro CR-PIT with ^{18}F-FDG by bioluminescence imaging. Five hundred thousand cells were seeded into 12-well plates and incubated for 24 h. After the cells were washed with PBS, 1 mL of phenol red free culture medium was added to each well. Ten micrograms of pan-IR700 for A431-luc and MDAMB468-luc cells or tra-IR700 for 3T3/HER2-luc cells containing medium were added to each well 0.5 h before ^{18}F-FDG was added. One milliliter of phenol red free culture medium was also added to each well after the medium was washed with PBS before the addition of ^{18}F-FDG. A shorter incubation time compared with UV-A PIT was selected because bioluminescence of cancer cells increases rapidly in a short time and only a 1-h incubation time with antibody-photoabsorber conjugate (APC) has been reported to induce cytotoxic effect due to NIR-PIT (*1*). For bioluminescence, 150 μg of D-luciferin (Gold Biotechnology) were added to each well and analyzed on a bioluminescence imaging system (Photon Imager; Biospace Lab) for luciferase activity −2 (2 h before), 0 (immediately after), 2, 4, 8, and 24 h after the addition of ^{18}F-FDG (the dose of ^{18}F-FDG was 0, 0.11, 0.37, 1.11, 3.7, and 11.1 MBq, respectively). Luciferase activity was reported in relative light units. Regions of interest of similar size were placed on each well encompassing the whole well, and the sum of relative light units was calculated using M^3 Vision Software (Biospace Lab). Next, the luciferase activity ratio was calculated from each value divided by baseline value.

Animal Model

We performed an animal study using only the A431-luc tumor model because clear CR-PIT effect was confirmed in vitro using this cell line. All procedures were performed in compliance with the *Guide for the Care and Use of Laboratory Animals* (*15*) and approved by NCI-Bethesda Animal Care and Use Committee. Six- to 8-wk-old female homozygote athymic nude mice were purchased from Charles River (National Cancer Institute). A431-luc cells (2×10^6 in PBS) were injected subcutaneously in the right dorsum of the mice under isoflurane anesthesia. Experiments were conducted at 5 d after cell injection.

In Vivo CR-PIT with ^{18}F-FDG

Tumor-bearing mice were randomized into 4 groups of at least 10 animals per group for the following treatments: no treatment (control); 200 μg of pan-IR700 intravenously (APC intravenously only); 37 MBq of ^{18}F-FDG injection only (^{18}F-FDG only); and 200 μg of pan-IR700 intravenously, and 37 MBq of ^{18}F-FDG were administered on day 1 after injection of APC (CR-PIT). This ^{18}F-FDG dose was selected because 37 MBq was the maximum dose that can be given to a mouse without inducing cytotoxic effects in the A431-luc tumor cells (data not shown).

Under anesthesia, tumor-bearing mice were administered 37 MBq of ^{18}F-FDG intravenously. All injections of ^{18}F-FDG were performed in the late morning with fasting from the evening before as that can affect the ^{18}F-FDG biodistribution (*16*). At 5 h after ^{18}F-FDG injection, the mice were imaged under anesthesia with 2%–3% isoflurane using BioPET/CT (Bioscan Inc.) to confirm biologic uptake. This time was selected to allow sufficient decay because the maximum dose of ^{18}F-FDG that still provides accurate measurement on this scanner is around 11.1 MBq. Both PET and CT imaging data were acquired. The PET images were acquired using an energy window of 250–700 keV. The PET images were reconstructed using a Fourier rebinning algorithm to generate 2-dimensional sinograms from the 3-dimensional list-mode data. The sinograms were corrected for randoms, scatter, and detector normalization artifacts. CT-based attenuation correction was also applied to the sinograms. The fully corrected sinograms were reconstructed into images using an ordered-subset expectation maximization algorithm. CT images of the mice were acquired using an x-ray tube voltage and current settings of 50 kV and 180 mA, respectively, and reconstructed using a filtered backprojection algorithm.

The treatment effects were determined with relative bioluminescence measured before and after treatment. For bioluminescence, D-luciferin (15 mg/mL, 200 μL) was injected intraperitoneally and the

mice were analyzed with a Photon Imager for luciferase activity before and 8 and 24 h after ^{18}F-FDG injection. Regions of interest of similar size were placed over each tumor.

Hepatotoxicity Induced by CR-PIT with ^{18}F-FDG

Hepatotoxicity may result from CR-PIT due to accumulating both ^{18}F-FDG and APC in the liver. To validate the degree of hepatotoxicity due to CR-PIT, mice were randomized into 4 groups with at least 2 animals per group for the following treatments: no treatment (control); 300 μg of pan-IR700 intravenously (APC intravenously only); 300 μg of pan-IR700 intravenously and then 40 J/cm^2 of NIR light exposed to the liver on day 1 after injection of APC (NIR-PIT); and 300 μg of pan-IR700 intravenously, and 111 MBq of ^{18}F-FDG were administered on day 1 after injection of APC (CR-PIT). NIR light was exposed to the liver using NIR laser light at a 685- to 693-nm wavelength (BWF5-690-8-500-0.37; B&W TEK Inc.) while the remainder of the body was shielded from light with aluminum foil.

Pathologic Analysis for Treated Tumor and Liver

To evaluate histologic changes after CR-PIT, light microscopy was performed using an Olympus BX61 microscope (Olympus America, Inc.). A431-luc tumors were excised from control mice, 24 h after injection of pan-IR700 (APC intravenously only), 24 h after injection of ^{18}F-FDG (^{18}F-FDG only), and 24 h after CR-PIT. Livers were also removed from control mice, 24 h after injection of pan-IR700 (APC intravenously only), 24 h after NIR-PIT, and 24 h after CR-PIT. Tumors and livers were placed in 10% formalin, and serial 10-μm slice sections were fixed on glass slides with hematoxylin and eosin staining.

Statistical Analysis

Statistical analysis was performed with JMP 10 software (SAS Institute). Data are expressed as mean ± SEM from a minimum of 4 experiments, unless otherwise indicated. We determined the differences in each percentage of surviving cells compared with the value without UV-A light or APC (control) using Dunnett correction for multiple comparison. For evaluation of luciferase activity, we also determined each luciferase activity ratio compared with the value at starting point for in vitro and controls (group 1) in vivo using Dunnett correction for multiple comparison. Differences of $P < 0.05$ were considered statistically significant.

RESULTS

In Vitro UV-A PIT

A431-Luc Cells. The percentage of surviving cells decreased in a light dose-dependent manner ($P < 0.01$ for 0.025, 0.05, 0.1, 0.2, 0.4, 0.8, and 1.6 J/cm^2 of UV-A light with pan-IR700 compared with the value without UV-A light or pan-IR700) (Fig. 2A). However, significant cytotoxicity associated with UV-A light alone (over 0.8 J/cm^2) was seen in the absence of pan-IR700 and with pan-IR700 alone but no UV-A light (Fig. 2A). The Δ percentage of surviving cells increased in a light dose-dependent manner with pan-IR700 whereas Δ percentage of surviving cells was negligible up to 0.4 J/cm^2 of UV-A light irradiation without pan-IR700. Thus, we concluded that UV-A light with pan-IR700 induces cell death because of the photoimmunotherapy effect (Supplemental Fig. 1; supplemental materials are available at http://jnm.snmjournals.org).

MDAMB468-Luc Cells. The percentage of surviving cells decreased in a light dose-dependent manner ($P = 0.11$ for 0.025 J/cm^2, $P < 0.01$ for 0.05, 0.1, 0.2, 0.4, 0.8, and 1.6 J/cm^2 of UV-A light with pan-IR700 compared with the value without UV-A light or pan-IR700) (Fig. 2B). However, significant cytotoxicity associated with UV-A light alone in the absence of pan-IR700 was observed ($P < 0.01$ for 0.1, 0.2, 0.4, 0.8, and 1.6 J/cm^2 compared with the value without UV-A light or pan-IR700) (Fig. 2B).

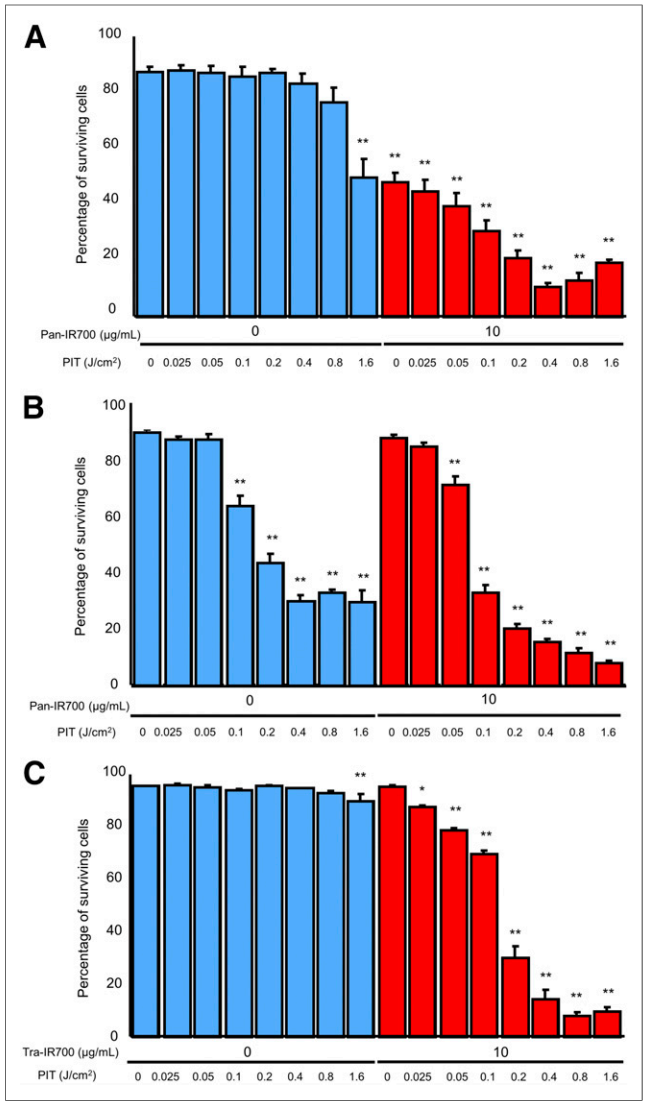

FIGURE 2. Evaluation of in vitro UV-A PIT (*$P < 0.05$, **$P < 0.01$, vs. untreated control). (A) Percentage of surviving cells decreased in light dose-dependent manner although 50% of A431-luc cells died when pan-IR700 alone without UV-A light was administered. (B) Propidium iodide staining showed membrane damage in MDAMB468-luc cells induced by UV-A PIT although significant cytotoxicity associated with UV-A light alone was observed. (C) With tra-IR700, percentage of surviving 3T3/HER2-luc cells decreased in light dose-dependent manner.

3T3/HER2-Luc Cells. The percentage of surviving cells decreased in a light dose-dependent manner ($P = 0.04$ for 0.025 J/cm^2, $P < 0.01$ for 0.05, 0.1, 0.2, 0.4, 0.8, and 1.6 J/cm^2 of UV-A light with tra-IR700 compared with the value without UV-A light or tra-IR700) (Fig. 2C). There was no significant cytotoxicity associated with UV-A light alone up to 0.8 J/cm^2 in the absence of tra-IR700 compared with without UV-A light or tra-IR700.

In Vitro CR-PIT with ^{18}F-FDG

A431-Luc Cells. There was no significant difference in luciferase activity ratio between 0 and −2 h with pan-IR700 and ^{18}F-FDG ($P = 0.09$, 0.42, 0.38, 0.27, and 0.64 for 0.11, 0.37, 1.11, 3.7,

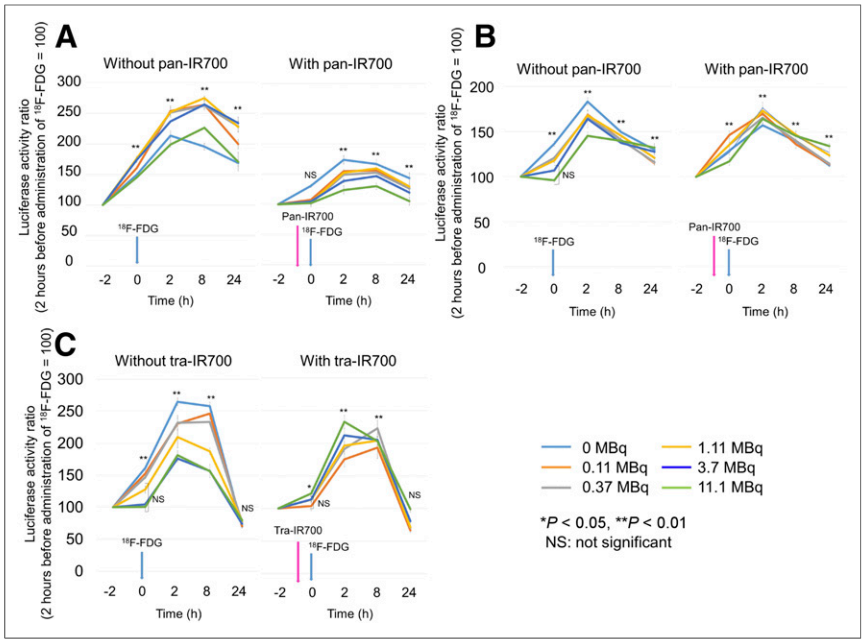

FIGURE 3. Evaluation of in vitro CR-PIT using ^{18}F-FDG. (A) When A431-luc cells were used, suppression of luciferase activity in cells was seen in CR-PIT and the degree of suppression increased in a dose-dependent manner. (B) When MDAMB468-luc cells were used, CR-PIT did not significantly change the level of luciferase activity compared with ^{18}F-FDG alone. (C) When 3T3/HER2-luc cells were used, CR-PIT also did not significantly change the level of luciferase activity compared with ^{18}F-FDG alone.

and 11.1 MBq of ^{18}F-FDG administration, respectively) (Fig. 3A). Luciferase activity ratio increased significantly at 2, 8, and 24 h after ^{18}F-FDG administration compared with that at −2 h with and without ^{18}F-FDG ($P < 0.01$ for all). On the other hand, without pan-IR700 luciferase activity ratio increased significantly at all time points including 0 h compared with that at −2 h regardless of presence or absence of ^{18}F-FDG ($P < 0.01$ for all) (Fig. 3A). Taken together, CR-PIT from ^{18}F-FDG had a demonstrable effect on A431-luc cells in vitro.

MDAMB468-Luc Cells. In the absence of pan-IR700, luciferase activity ratio increased significantly at 0 h compared with that at −2 h up to 1.11 MBq of ^{18}F-FDG administration ($P < 0.01$ for 0, 0.11, 0.37, and 1.11 MBq of ^{18}F-FDG administration, respectively), whereas there was no significant difference in luciferase activity ratio between 0 and −2 h when the dose was increased to 3.7 or 11.1 MBq of ^{18}F-FDG ($P = 0.37$ and 0.97 for 3.7 and 11.1 MBq of ^{18}F-FDG administration, respectively) (Fig. 3B). Moreover, when pan-IR700 was given, luciferase activity ratio increased significantly at all time points including 0 h compared with that at −2 h with and without ^{18}F-FDG ($P < 0.01$ for all) (Fig. 3B). These results suggested that the effect of CR-PIT could not be observed in vitro using MDAMB468-luc cells.

3T3/HER2-Luc Cells. In the absence of tra-IR700, luciferase activity ratio increased significantly at 0 h compared with that at −2 h up to 0.37 MBq of ^{18}F-FDG administration ($P < 0.01$ for 0, 0.11, and 0.37 MBq of ^{18}F-FDG administration, respectively), whereas there was no significant difference in luciferase activity when more than 1.11 MBq of ^{18}F-FDG were administered ($P = 0.05$, 0.58, and 0.78 for 1.11, 3.7, and 11.1 MBq of ^{18}F-FDG administration, respectively) (Fig. 3C), suggesting that cytotoxicity might be induced by CR derived from ^{18}F-FDG in vitro. In the presence of tra-IR700, luciferase activity increased significantly with administration of 11.1 MBq of ^{18}F-FDG ($P = 0.03$), although there was no significant difference in luciferase activity ratio between 0 and −2 h with administration of ^{18}F-FDG up to 3.7 MBq ($P = 0.71$, 0.24, 0.19, and 0.20 for 0.11, 0.37, 1.11, and 3.7 MBq of ^{18}F-FDG administration, respectively) (Fig. 3C). Thus, the effect of CR-PIT was unpredictable in vitro using 3T3/HER2-luc cells.

In Vivo CR-PIT with ^{18}F-FDG

The treatment regimen is shown in Figure 4A. ^{18}F-FDG clearly accumulated within the tumor (Fig. 4B). In the control, APC-intravenously-only, and ^{18}F-FDG–only groups luciferase activity of tumors increased rapidly with time, indicating tumor growth. On the other hand, in the CR-PIT group luciferase activity of tumors increased at a lower rate (Figs. 4C and 5A). Eight hours after ^{18}F-FDG injection, the post–/pre–^{18}F-FDG luciferase activity ratio in the CR-PIT group was significantly lower than that in the control group, whereas there was no significant difference in luciferase activity in APC-intravenously-only and ^{18}F-FDG–only groups compared with controls ($P = 0.83$, 0.54, and 0.04 for APC-intravenously-only, ^{18}F-FDG–only, and CR-PIT groups, respectively) (Fig. 5B). Twenty-four hours after ^{18}F-FDG injection post–/pre–^{18}F-FDG luciferase activity ratio in the CR-PIT group was also significantly lower than that in controls ($P = 0.05$). However, there was no significant difference in luciferase activity in APC-intravenously-only and ^{18}F-FDG–only groups compared with controls ($P = 0.47$ and 0.85 for APC intravenously only and ^{18}F-FDG only, respectively) (Fig. 5B).

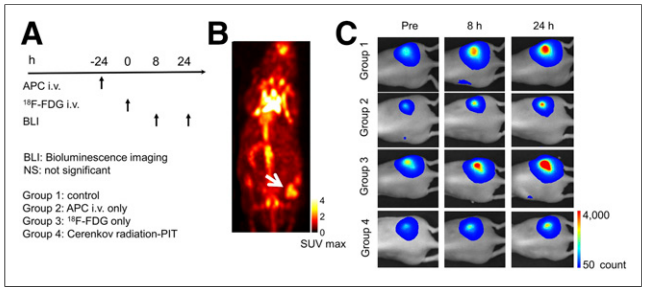

FIGURE 4. In vivo effect of CR-PIT on A431-luc tumor. (A) CR-PIT regimen is shown. (B) ^{18}F-FDG PET imaging of tumor-bearing mice. Tumor showed high accumulation of ^{18}F-FDG (arrow). (C) Bioluminescence imaging of tumor-bearing mice.

Pathologic Analysis for Treated Tumor and Liver

CR-PIT–treated tumors showed cellular necrosis and microhemorrhage within a background of live but damaged tumor cells whereas little damage was observed in tumors receiving ^{18}F-FDG only (Fig. 6). This appearance is similar but milder to that

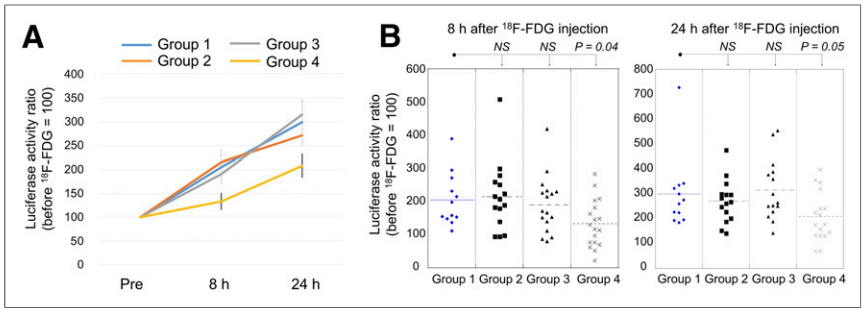

FIGURE 5. In vivo effect of CR-PIT on A431-luc tumor. (A) Luciferase activity ratio was suppressed in CR-PIT group compared with control group. (B) Significant suppression of luciferase activity ratio was seen in CR-PIT group compared with control group. NS = not significant.

observed with conventional NIR-PIT. No obvious damage was observed in tumors in the APC-intravenously-only and control groups (Fig. 6).

The livers treated with NIR-PIT showed yellowish color changes on the surface in macroscopic appearance and extensive hepatic cell damage especially at the peri-Glisson's capsule area on microscopic images (Supplemental Fig. 2). On the other hand, the livers treated with CR-PIT showed mild hepatic cell damage mainly at the peri-Glisson's capsule area on microscopic images; however, there was no obvious change in macroscopic surface appearance. No obvious damage was observed in the livers in the APC-intravenous-only and control groups (Supplemental Fig. 2).

DISCUSSION

From our results, we found that UV-A light can induce photoimmunotherapy. However, some cells are quite sensitive to the effects of UV-A light alone as shown in MDAMB468-luc cells, suggesting that some cancer cells (as well as normal cells) are highly sensitive to UV-A light by itself whereas NIR light is completely harmless by itself (*1,17,18*).

The in vitro results of CR-PIT suggested that among the cells tested, A431-luc cells were more sensitive than MDAMB468-luc and 3T3/HER2-luc cells. This may be because CR and radiation exposure itself may induce variable cytotoxicity in certain cell lines (*19*), resulting in reduced additional cytotoxic effects of CR-PIT. Variability in this effect may be traced to variable accumulation of ^{18}F-FDG in each cell type (*20*). Alternatively, the light produced by CR may be insufficient to induce photoimmunotherapy effects in these cell lines.

CR-PIT for A431-luc tumor showed significant inhibition of luciferase activity in vivo. Moreover, pathologic analysis revealed cellular necrosis and microhemorrhage within the CR-PIT–treated tumor, indicating that CR-PIT was capable of inhibiting A431-luc tumor growth.

The decrease of luciferase activity after CR-PIT in A431-luc tumors was not observed consistently over the entire time course of the experiment unlike NIR-PIT (*1*). This suggests CR-PIT was less effective than NIR-PIT. First, photoimmunotherapy depends on light absorption by the photoabsorber IR700, which is optimally excited at 689 nm. UV-A light at 350 nm is only one-third as effective as NIR. Furthermore, compared with NIR, CR is much lower in intensity and penetrates only 1–2 mm into tissue. Moreover, CR is emitted inside of the cell and lipid cell membrane has the capacity to absorb UV light including CR (*13,20*). Therefore, only a small part of CR may reach IR700 on the cell membrane (*1*).

One approach would be to inject a larger dose of ^{18}F-FDG with proportionately more CR. However, one is limited by the permissible radiation dose in humans. Moreover, hepatotoxicity could result from CR-PIT in the liver due to accumulation of both ^{18}F-FDG and APC. Mild hepatic cell damage was observed in peri-Glisson's capsule area; however, this damage was diffuse throughout the liver, suggesting potential for significant hepatotoxicity. Therefore, in the future, it might be preferable to select PET agents and Ab-IR700 conjugates that demonstrate less hepatic uptake than ^{18}F-FDG or pan-IR700.

Selecting an alternative radionuclide that emits high-energy β-radiation with high-yield CR is a potential way to improve the effect of CR-PIT (*6,12,21,22*). However, the labeled agent must be highly tropic to cancer with little off-target accumulation and the half-life and dosimetry must be such that acceptable exposure to nontarget organs can be achieved while still producing enough light for CR-PIT.

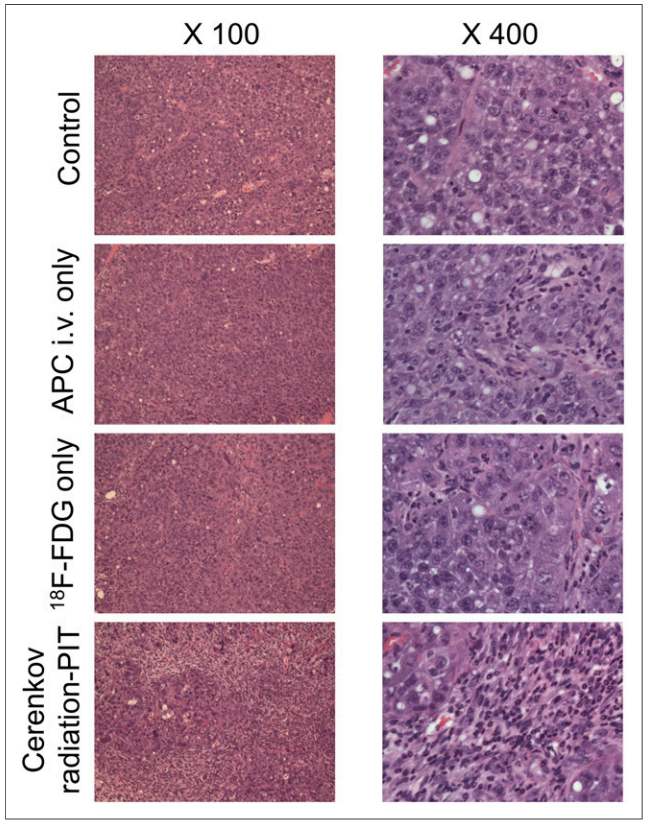

FIGURE 6. Resected tumors stained with hematoxylin and eosin. Cellular necrosis and microhemorrhage were seen within a background of live but damaged tumor cells after CR-PIT whereas little damage was observed in tumors receiving ^{18}F-FDG administration alone. No obvious damage was observed in the tumor receiving only APC but no ^{18}F-FDG administration.

CR-activated photosensitizer-labeled nanoparticles have been reported (*8,23,24*). However, unlike NIR-PIT, none of photosensitizer-labeled nanoparticles has been used in clinical trials. Another concern with CR-activated photosensitizer-labeled nanoparticles is inferior selectivity because the CR emitted from these nanoparticles cannot be directed exclusively to the tumor area (*1*). In contrast NIR-PIT is highly selective for tumor. Thus, we think CR-PIT may be a better approach than CR-activated photosensitizer-labeled nanoparticles.

Because CR-PIT has less immediate efficacy compared with NIR-PIT, we did not conduct a long-term evaluation as tumors regrew quickly, resulting in no significant therapeutic effect. However, CR clearly induced cytotoxic photoimmunotherapy in vivo, indicating that, similar to NIR-PIT, CR-PIT has the potential to activate anticancer host immunity by inducing immunogenic cell death either using CR-PIT or using an antibody-conjugate that selectively targets tumor-associated regulatory T cells (*2,25*).

CONCLUSION

CR-PIT using ^{18}F-FDG showed significant therapeutic effects when using A431-luc cells in vitro and in vivo. Although CR-PIT is less effective than NIR-PIT, it could nevertheless have an impact for treating tumors located deep within the body where NIR light cannot reach. Specific developments that might aid the effectiveness of CR-PIT include the development of specific radioactive probes that emit more CR but have lower hepatic accumulation.

DISCLOSURE

This research project has been funded in whole with federal funds from the National Cancer Institute, National Institutes of Health, under Intramural Research Program and contract no. HHSN261200800001E. The content of this publication does not necessarily reflect the views or policies of the Department of Health and Human Services, nor does mention of trade names, commercial products, or organizations imply endorsement by the U.S. government. No other potential conflict of interest relevant to this article was reported.

ACKNOWLEDGMENTS

We thank Anita Ton Thien for reconstruction of PET images and Philip C. Eclarinal for management of ^{18}F-FDG.

REFERENCES

1. Mitsunaga M, Ogawa M, Kosaka N, Rosenblum LT, Choyke PL, Kobayashi H. Cancer cell-selective in vivo near infrared photoimmunotherapy targeting specific membrane molecules. *Nat Med.* 2011;17:1685–1691.
2. Ogawa M, Tomita Y, Nakamura Y, et al. Immunogenic cancer cell death selectively induced by near infrared photoimmunotherapy initiates host tumor immunity. *Oncotarget.* 2017;8:10425–10436.
3. Ai X, Mu J, Xing B. Recent advances of light-mediated theranostics. *Theranostics.* 2016;6:2439–2457.
4. Hudson DE, Hudson DO, Wininger JM, Richardson BD. Penetration of laser light at 808 and 980 nm in bovine tissue samples. *Photomed Laser Surg.* 2013;31:163–168.
5. Cerenkov PA. Visible emission of clean liquids by action of γ radiation. *Doklady Akademii Nauk SSSR.* 1934;2:451–454.
6. Thorek DL, Robertson R, Bacchus WA, et al. Cerenkov imaging - a new modality for molecular imaging. *Am J Nucl Med Mol Imaging.* 2012;2:163–173.
7. Robertson R, Germanos MS, Li C, Mitchell GS, Cherry SR, Silva MD. Optical imaging of Cerenkov light generation from positron-emitting radiotracers. *Phys Med Biol.* 2009;54:N355-365.
8. Shaffer TM, Drain CM, Grimm J. Optical imaging of ionizing radiation from clinical sources. *J Nucl Med.* 2016;57:1661–1666.
9. Thorek DL, Riedl CC, Grimm J. Clinical Cerenkov luminescence imaging of ^{18}F-FDG. *J Nucl Med.* 2014;55:95–98.
10. Zhang X, Kuo C, Moore A, Ran C. In vivo optical imaging of interscapular brown adipose tissue with ^{18}F-FDG via Cerenkov luminescence imaging. *PLoS One.* 2013;8:e62007.
11. Spinelli AE, D'Ambrosio D, Calderan L, Marengo M, Sbarbati A, Boschi F. Cerenkov radiation allows in vivo optical imaging of positron emitting radiotracers. *Phys Med Biol.* 2010;55:483–495.
12. Liu H, Ren G, Miao Z, et al. Molecular optical imaging with radioactive probes. *PLoS One.* 2010;5:e9470.
13. Warburg O. On the origin of cancer cells. *Science.* 1956;123:309–314.
14. Lin H, Zhang R, Gunn JR, et al. Comparison of Cherenkov excited fluorescence and phosphorescence molecular sensing from tissue with external beam irradiation. *Phys Med Biol.* 2016;61:3955–3968.
15. *Guide for the Care and Use of Laboratory Animals.* Washington, DC: National Academy Press; 1996.
16. Lee KH, Ko BH, Paik JY, et al. Effects of anesthetic agents and fasting duration on ^{18}F-FDG biodistribution and insulin levels in tumor-bearing mice. *J Nucl Med.* 2005;46:1531–1536.
17. Sinha RP, Hader DP. UV-induced DNA damage and repair: a review. *Photochem Photobiol Sci.* 2002;1:225–236.
18. Rastogi RP, Richa, Kumar A, Tyagi MB, Sinha RP. Molecular mechanisms of ultraviolet radiation-induced DNA damage and repair. *J Nucleic Acids.* 2010;2010:592980.
19. Malaise EP, Fertil B, Chavaudra N, Guichard M. Distribution of radiation sensitivities for human tumor cells of specific histological types: comparison of in vitro to in vivo data. *Int J Radiat Oncol Biol Phys.* 1986;12:617–624.
20. Pauwels EK, Sturm EJ, Bombardieri E, Cleton FJ, Stokkel MP. Positron-emission tomography with [^{18}F]fluorodeoxyglucose. Part I. Biochemical uptake mechanism and its implication for clinical studies. *J Cancer Res Clin Oncol.* 2000;126:549–559.
21. Ruggiero A, Holland JP, Lewis JS, Grimm J. Cerenkov luminescence imaging of medical isotopes. *J Nucl Med.* 2010;51:1123–1130.
22. Beattie BJ, Thorek DL, Schmidtlein CR, Pentlow KS, Humm JL, Hielscher AH. Quantitative modeling of Cerenkov light production efficiency from medical radionuclides. *PLoS One.* 2012;7:e31402.
23. Kotagiri N, Sudlow GP, Akers WJ, Achilefu S. Breaking the depth dependency of phototherapy with Cerenkov radiation and low-radiance-responsive nanophotosensitizers. *Nat Nanotechnol.* 2015;10:370–379.
24. Kamkaew A, Cheng L, Goel S, et al. Cerenkov radiation induced photodynamic therapy using chlorin e6-loaded hollow mesoporous silica nanoparticles. *ACS Appl Mater Interfaces.* 2016;8:26630–26637.
25. Sato K, Sato N, Xu B, et al. Spatially selective depletion of tumor-associated regulatory T cells with near-infrared photoimmunotherapy. *Sci Transl Med.* 2016;8:352ra110.